FERMILAB-CONF-19-375-AD

Magnetic Field Mapper

Ben Sims

Michigan State University

Mentor – Jonathan Jarvis

Lee Teng Internship

August 14, 2019

Iota Fast Facility

This manuscript has been authored by Fermi Research Alliance, LLC under Contract No. DE-AC02-07CH11359 with the U.S. Department of Energy, Office of Science, Office of High Energy Physics.

TABLE OF CONTENTS

INTRODUCTION

The scientific program at the Integrable Optics Test Accelerator (IOTA) ring depends on a wide variety of specialized magnets, and validation of their field quality is important for ensuring proper performance. A number of these magnetic elements have both high field quality and a small physical aperture, and adequate field-mapping solutions have not been readily available in house or with external vendors. To solve this problem, a new magnetic-field mapping device needs to be developed. This new system features a high-precision tesla-meter, with a low-profile three-axis Hall probe, and stepper motors to allow for high-speed, accurate positioning of the probe. This new Magnetic Field Mapper (MFM), shown in Figure 1, will be capable of quickly mapping a wide variety of magnets to high precision, thus eliminating the need to send magnets off-site for expensive and time-consuming mapping.

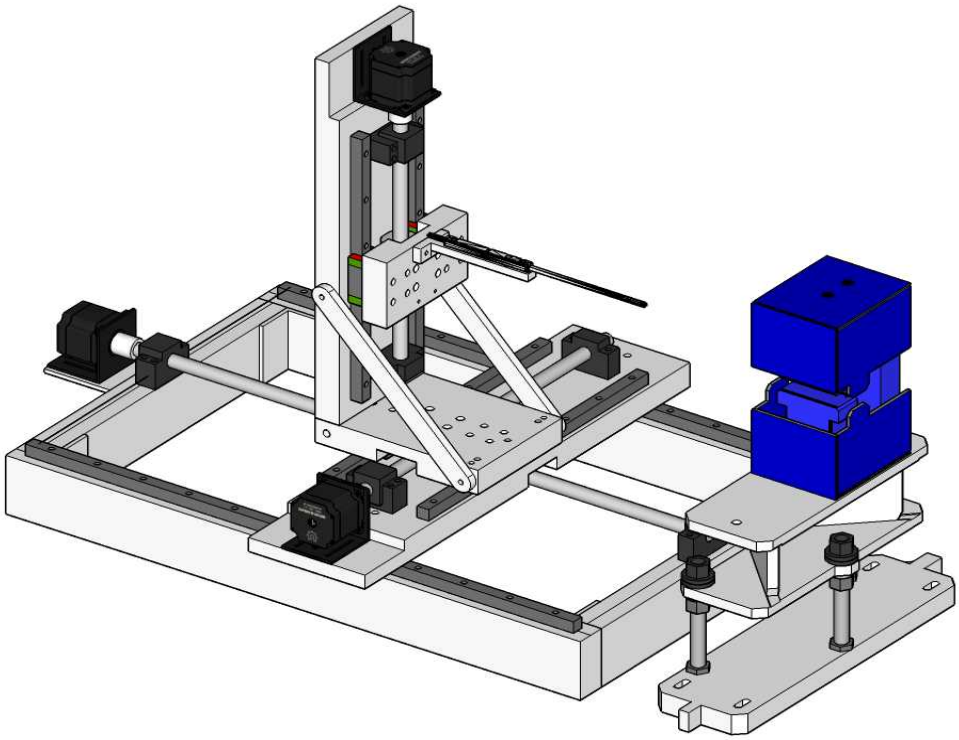

Figure 1. Solid model of the MFM with an optical stochastic cooling chicane dipole, In blue, for scale. The longitudinal axis of the system is ~0.6 m in length.

COORDINATE SYSTEM

The coordinate system for the MFM differs from the standard accelerator coordinate system. The probe used in this system has its own coordinate system that everything else was set up to match. Figure 2 shows the coordinate system in relation to the probe. The X-Axis is the vertical coordinate, the Y-Axis is the horizontal transverse coordinate, and the Z-Axis is the horizontal coordinate. The positive direction is in the direction of the arrow, opposing the arrow is negative. This new coordinate system differs from the standard accelerator frame as X and Y are flipped. To convert to a standard frame $X_{MFM} = -Y_{Standard}$ and $Y_{MFM} = X_{Standard}$. The reason for sticking with this adapted frame was that the probe sends data in a specific order; Magnitude, X, Y, Z. In order to avoid any confusion thought the code and documentation, this coordinate system is maintained to match the probe data. This data can then be easily analyzed in the standard frame using the axis conversions above to change it into the more conventional frame.

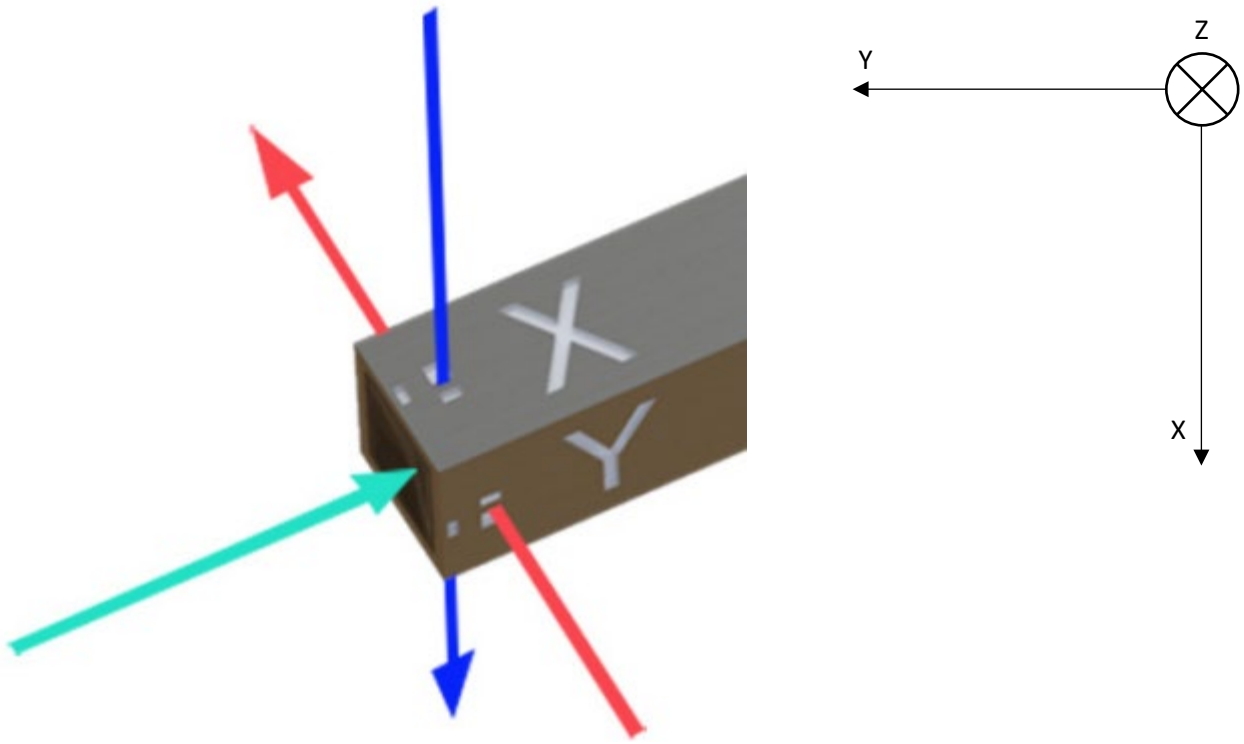

Figure 2. MFM Coordinate system

APPROACH

When building the MFM special importance was given to two key aspects functionality and flexibility. This new device needs to be easy enough to use that with documentation this device could be able to be used by anyone. Second, this system needed to have the flexibility that industry lacked. This means being able to map not only a wide variety of sizes but also different strength magnetic fields. To accomplish these goals the Magnetic Field Mapper consists of three main systems: motion, measurement, and control. Each of these overarching systems contains many subsystems and components that will now be discussed.

Controls

The motion and measurement systems will be connected to a Raspberry Pi for control and acquisition of data. Using custom Python scripts, a unique mesh of points can be generated for a variety of magnet shapes and sizes. The Raspberry Pi will then turn that path into a list of steps that it will send to the stepper motors. Following the stepper motors moving to a new position the Teslameter will take and report data back to the Pi and compile a list of the data. This process will then be repeated until the desired space has been mapped.

Raspberry Pi 3B+

The Raspberry Pi is a Linux based computer that was chosen because of its GPIO output pins. These pins allow for easy communication to the stepper drivers as they can be controlled using simple python scripts. Being able to control the stepper drivers was a critical feature that the chosen computer needed to have. As very few computers have such an easy way of sending data as the Raspberry Pi, it was an easy choice. The Raspberry Pi also had a wide variety of options for interfacing with the measurement devices which

was important as it is a Linux device and ensuring driver compatibility between different devices can be a challenge. The ports used on the Raspberry Pi include the Ethernet port for the Teslameter and 6 of the GPIO pins.

GPIO Breakout

The GPIO pins from the Raspberry Pi were extended into a custom 3D printed enclosure. Reference figure 2 shows the fully wired up device. Inside on a breadboard, the desired connections were made and soldered into place. Nine pairs of twisted cables were run out of three different holes in the lid. This was done to lower the chance of cross-talk between the wires. These wires were then run to the stepper Drivers. The switch on the side of the enclosure is for enabling and disabling the stepper drivers.

Python

All the code used throughout this project are custom scripts written explicitly to run this system. However, because of the low processing power of the Raspberry Pi, some work needs to be done on a more powerful computer.

Pre-Raspberry PI

This portion of the code needs to run on something more powerful than the Pi. During this portion of the code development, a mesh of points is built. This mesh as some special features that make it optimized for this project. First, it creates the mesh so that there is little time wasted moving the probe between successive points. This can be seen when a line scan is completed and instead of returning to the front and taking another scan it simply moves perpendicularly and takes the next line scan the opposite direction of the previous one. The second feature that helps reduce the duration of the scan and lower the point total is a double Gaussian distribution of points. When designing the density function a feature was added which allows the user to create regions of high and low density by moving the peaks of two separate Gaussian curves along the desired length of the scan. By making the density higher in more important regions of the scan as opposed to constant the resulting mesh has fewer points overall. This feature of the mesh can be used at points of interest like outside the magnet to detect fringe fields or at the edge of the magnet when the field is rapidly changing. The final step before loading the mesh grid on to the Pi is to turn the list of X, Y, Z coordinates into a list of X, Y, Z Steps that the Pi can use to control the stepper motors. Once all of this is done the Steps.csv file needs to be transferred to the Pi.

On-Raspberry Pi

Once on the Raspberry Pi, the only code that needs to be run is On-Raspberry Pi.py. This code features several different functions custom-built for this project. The main functions are movement and measurement. Using these functions, the Pi can communicate with the stepper motor and Teslameter to accumulate data into a series of lists. Sleep commands are used to allow for the Teslameter to report accurate data, as it needs time to clear the buffered data it has stored before it can accurately report the field at the new location. Once the mapping is complete, usually around 0.5 seconds per point, the data in the lists is saved to a new file called BField.csv. This features a list of data about the field at every point including the magnitude and X, Y, and Z components of the field.

Post-Raspberry Pi

Once the BField.csv and Steps.csv files have been transferred from the Pi to a more powerful machine the data and steps can be used to construct a variety of different plots describing the field. The data can also be compared against theoretical data for a quality check of the field quality.

Motion

The movement of the integrated system will be controlled with a system of stepper motors and high-current stepper drivers. The movement system is based on low-cost linear bearings, linear rails and precision ball screws driven by stepper motors. The unified system will be mounted on a series of Aluminum plates supported on a base of 15mm by 30mm 8020 extruded aluminum.

CNC components

The use of DIY CNC components was decided upon as a means of having precise control of the motion at a low cost. One risk of using low cost approaches like this can be the quality of the received parts. To avoid this possibility, the parts will be tested and adjusted as need be before the final assembly to ensure that all parts fit and work as they should with little to no error.

Ball Screws

Using ball screws of different lengths allows for the MFM to be able to move over a large area. This is key in allowing for the flexibility to map large and small magnets. Even though smaller magnets will not utilize the full range of motion of each axis, having that movement is critical for much larger magnets or magnets of different geometries. With the Ball screws used on the MFM, the Z-Axis has a range of 60cm, The Y-axis has a range of 38 cm, and the X-Axis has a range of 27 cm.

Linear Rails

The linear rails are useful in supporting each axis. They will be attached to each ball screw via an Aluminum plate, they prevent the plate from twisting or otherwise moving in a way that would be undesirable. Each axis will have two linear rails on either side of the ball screw.

Stepper Motor and Drivers

Stepper motors are precision devices that allow you to take steps in either a positive or negative direction. When attached to a device like a ball screw they allow for a precise number of steps of the motor to be turned into a change in linear distance. We will be using stepper motors to run all the ball screws in the MFM. Controlling the stepper motors and requires an interfacing device called a stepper driver. The stepper driver receives information from the Raspberry Pi in pulse trains which it then converts into a current that turns the motor the desired number of steps.

Stepper Motor 23HS30-3004S

The stepper motor that was chosen is quite powerful for what it needs to accomplish. This was done so that there would be no concern about not being able to move the integrated system and so that the motor would be less likely to slip and miss a step as the motor would be under a low load and should have no problem keeping up.

Digital Stepper Motor Driver DM542S

The stepper drivers were chosen for their compatibility with the stepper motor. The stepper drivers are run off 3.7-Amp, 24-volt power supplies. The drivers have built in opto-isolation to reduce the risk of damage to the Pi. The stepper drivers are wired in common anode mode which can be found in the manual for more details. The stepper drivers are sent a train of pulses which it utilizes in different ways. First, it needs a signal to enable the driver. This is always set to active unless the motor needs to be moved manually in which case the switch on the enclosure can be flipped to disable the drivers. Second, the direction the motor should be moved must be sent. This is a long pulse that runs until the end of the motion in the required direction. Finally, the number of steps are sent as a set number of pulses equal to the number of steps that need to be taken. Each pulse is separated by a delay of 0.15 microseconds. All

these pulses are controlled by the Pi and when interpreted by the stepper allow for a precise number of steps to be executed resulting in linear movement in that axis.

Aluminum Plates

The entire MFM will be built on a frame of custom machined aluminum plates and 15mm by 30mm 8020 aluminum. This keeps the entire system at a low weight while still providing the strength needed to stop any undesired movement. The bottom axis or Z-axis for this system will be supported by a set of 15 by 30 8020 Aluminum. This will create a large base that is very strong and allows for the linear rails and ball screw to be easily mounted in the track of the 8020 with the use of T nuts. The next axis up, the Y-Axis, will be attached to an aluminum plate that is attached underneath, to the ball screw and linear rails of the Z-axis. The final axis, the X-Axis, will be again supported by its custom aluminum plate in the same way as the Y-axis plate. Finally, the 3-Axis probe will be mounted on its own aluminum plate that is attached to the X-axis. In the end, this allows for a stable structure that supports each axis as well as keeping the system as light as possible for the stepper motors.

Measurement

The measurements will be taken using an F71 3-Axis Teslameter. The F71 3-Axis Teslameter had many key features that made it optimal for use on this project. These features can be split into features of the 2 main parts of the Teslameter, The Teslameter itself, and the Probe.

3 Axis Probe

This probe features a compact profile of 4x4 mm which enables the mapping of magnets with small apertures. As wells as the ability to be mounted in a variety of way. This is key for ensuring that the probe isn't moving in any unexpected ways while taking data. The probe also features high resolution (< 1 ppm) and absolute accuracy (+/- 0.25%) over a large range of magnetic-field strength (~G to ~350 kG), increasing its utility across IOTA's experimental program.

F71 Teslameter

The F71 Teslameter by Lakeshore Cryotronics was chosen because of the probe which provides a wide range of functionality, as well the Teslameter ability to connect to a variety of computers. This is critical when running all controls through a Linux based system. There needed to be a variety of ways to connect as this would eliminate the possibility of an incompatible driver halting the project. In the end, the Teslameter was connected using the ethernet ports of the Raspberry Pi and Teslameter. Using TCP commands, communication with the Teslameter was achieved as well as data being successfully transmitted.

Current Status of Project

The MFM is currently in the final stages of being assembled. The only parts that are not currently in use and assembled are the 8020 Base and Aluminum frame. Due to the time needed to design and machine custom aluminum plates for specialized mounting. This project will not be fully completed within the 10-week time frame. However, all that remains is to assemble the integrated system once the plates arrive. To ensure all that remains is to assemble the system, a series of experiments were put forward in order to test the code and parts that are in house. These test would be used to check that the systems function as expected and to collect some preliminary data on the OSC Dipoles that can be compared to simulated OSC Dipole field to check if the system is indeed reading everything correctly.

RESULTS

Pre-Assembly Data

Prior to assembly of the fully integrated systems, there was a need to test both the mapping capabilities as well as the stepper motor precision. The mapping capabilities of the magnet were tested by 3D printing a mount for the X-Axis a performing several line scans through the magnet. The stepper motor was tested by using a dial gauge to check the distance traveled after a set number of steps was requested.

Magnetic Field Mapping Test

To test the integrated system before assembly, one of the optical stochastic cooling (OSC) dipole magnets was mapped with a series of line scans. The OSC Dipole was mapped using only the X-Axis, resulting in a line scan of the magnetic field. To attach the probe to the X-axis a custom 3D printed mount was made which allowed the probe to be moved to different Y positions across the dipole's aperture. The data for the magnetic field was taken by aligning the probe to roughly the center of the magnet then taking a line scan down the length of the magnet. This process was then repeated at the center, 3mm to the right, and 6 mm to the right. With the scan, being repeated 10 times at each location. This was in order to integrate the field of the magnet at each location and come up with a set of data that shows the overall deviation of the integrated magnetic field over the magnet. The line scans at 6mm are shown in figure 3, the OSC dipole is shown in figure 4, the scan positions in the aperture are shown in figure 5 and the integrated field error is shown in figure 6. The red line in figure 3 is the simulated magnetic field of the OSC Dipole.

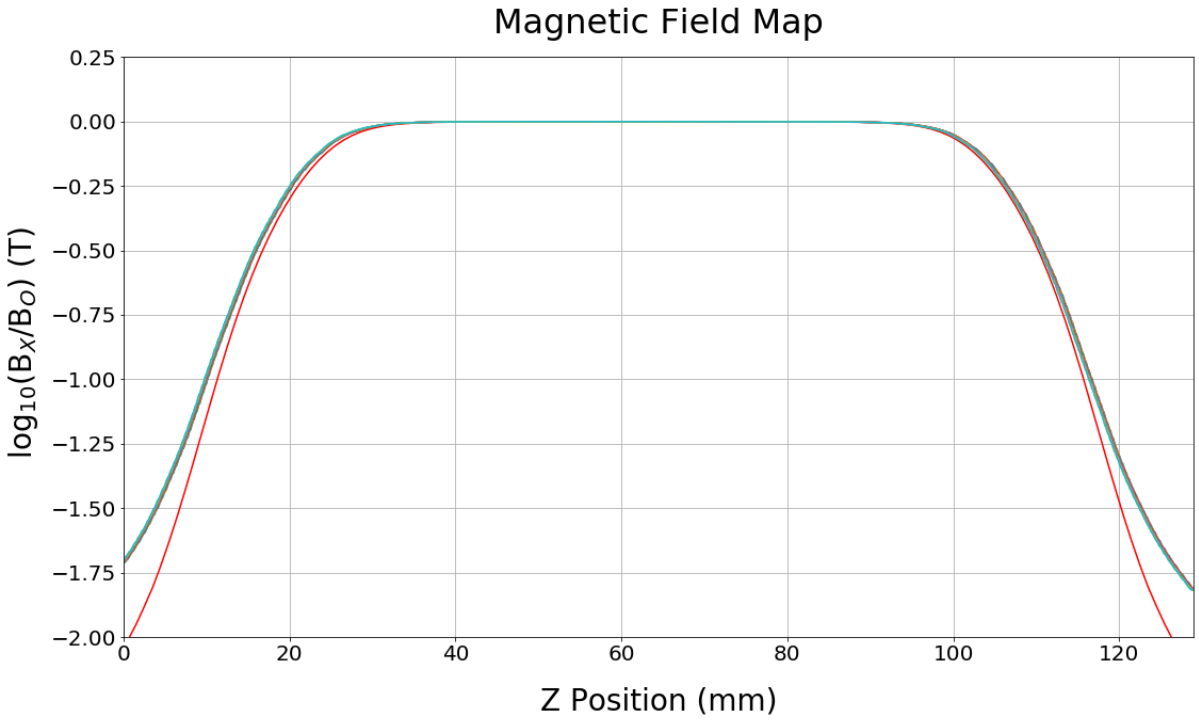

Figure 3. Line scan of magnetic field of OSC Dipole at 6mm

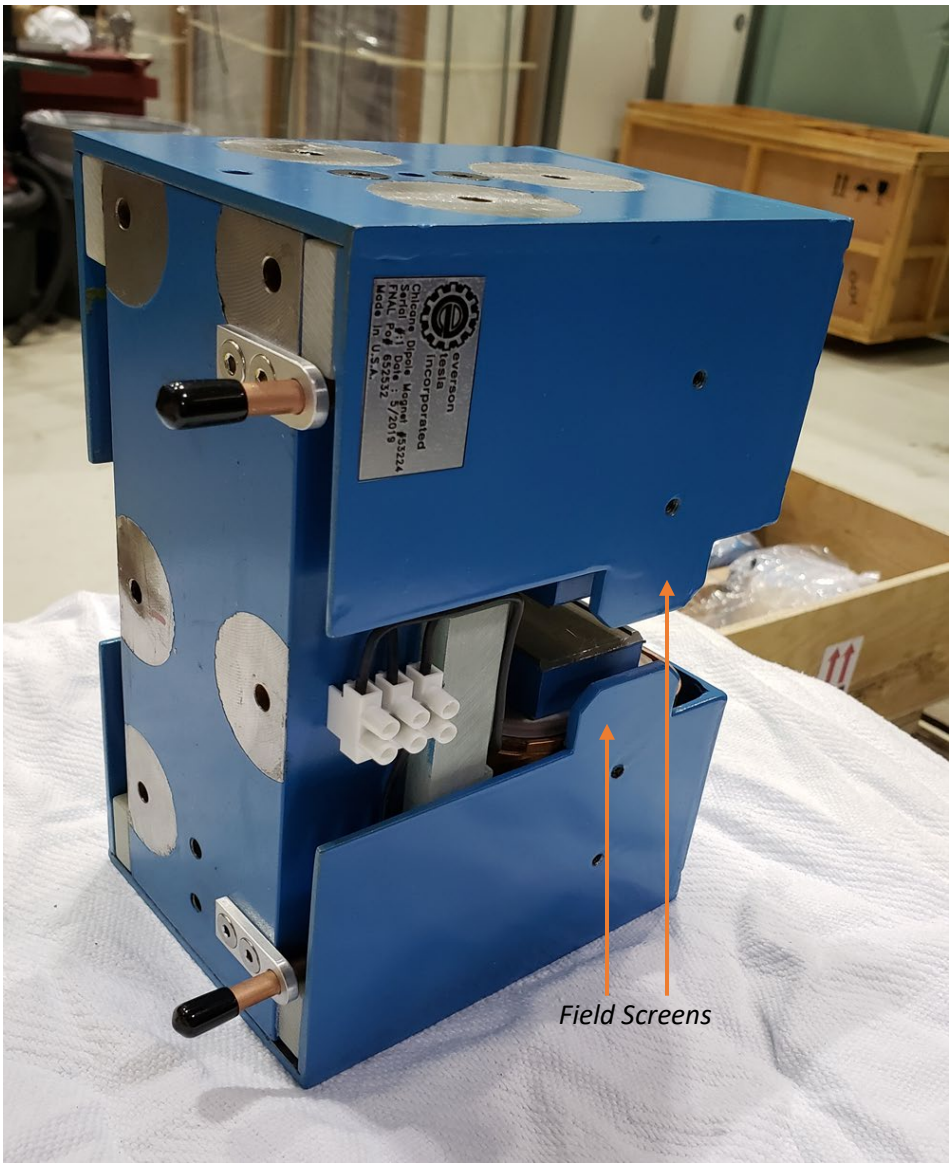

Figure 4. OSC Dipole

The magnetic field in all scans taken deviated from the simulated results outside of the field screens of the OSC Dipole. The field screens are in place in order to decrease the magnetic field outside of the magnet so that when the beam passes through the magnet it only interacts with the constant magnetic field. The deviation shown could have come from a variety of factors including; mount instability, inaccurate positioning of the probe, a bent ball screw, bent field screens, and/or a magnetized ball screw. These may all have been a factor in the data outside of the yoke of the magnet deviating from theory. However, these are expected to not be a problem for the integrated system as assembling the system should most of, if not all the possible sources of error except for the bent field screens and that is an important characteristic of the OSC dipole that the integrated system will be used to fix.

The integrated field error of the OSC dipole was measured to see if the OSC dipole was as uniform as was required when it was designed. The 2 dashed lines in figure 6 show the integrated field error at full aperture (~6mm) for the expected manufacturing tolerances. While some data falls in this range there are

many data points outside this region. The curved lines surrounding the data points indicate the concentration of data in that area. The wider the curve the more points in that area. The number of points outside the acceptable region may indicate an issue with the integrated field quality but more likely it is a result of errors in the field measurement system that were previously discussed. Once the Integrated system is fully assembled and systematics are fully characterized, the integrated field error can be rechecked to see it is within expected tolerances. The error is expected to decrease when fully assembled as once constrained the probe will no longer be able to move unexpectedly. When on the 3d printed mount the probe was able to move in the y and z plane slightly as it was not fully constrained. An additional point of note is that the trend in the data would indicate that the initial position of the probe was not centered at 0mm. As a result, the 0mm position, while used as a reference for all other points, is not the center of the magnetic field and the true magnetic center lies somewhere between the 0mm and 3mm data. Furthermore, vertical centering and alignment of the magnetic axis with the probe axis could not be assured in this initially testing.

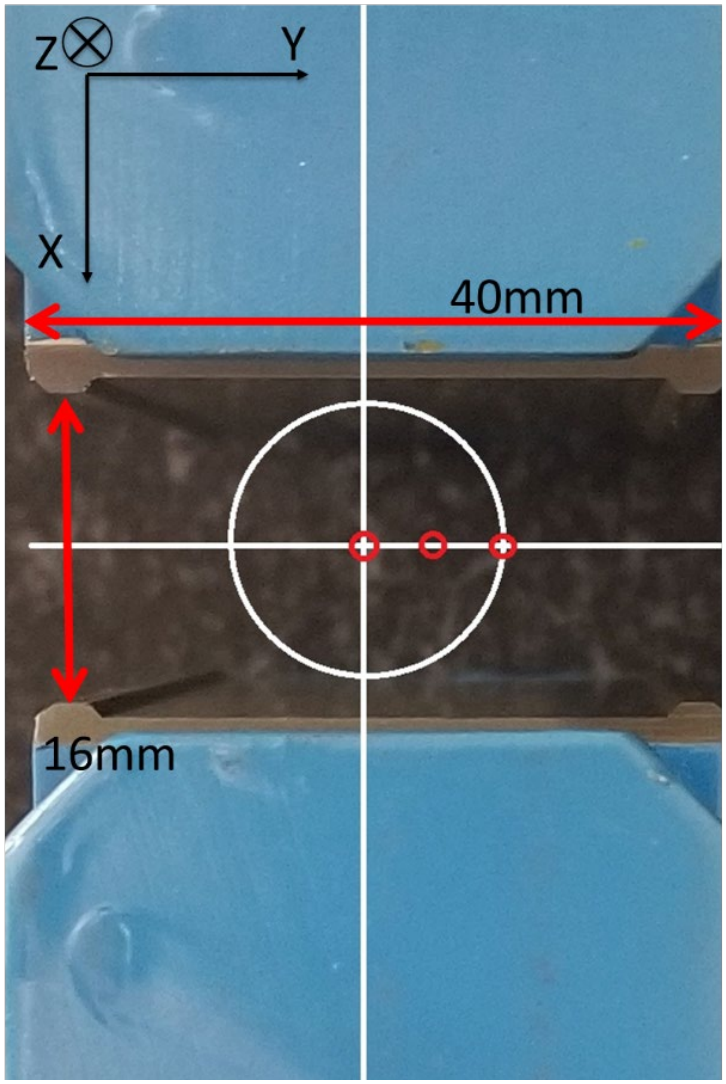

Figure 5. OSC Dipole Showing scan location. White circle indicates approximate aperture of 6.5mm

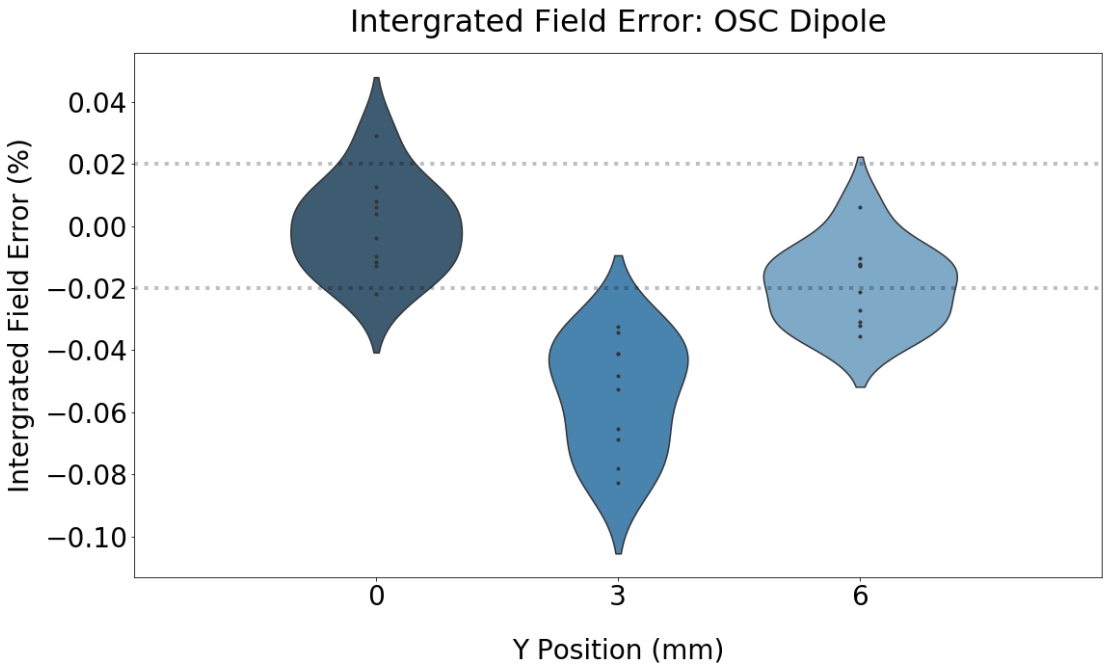

Figure 6. Integrated Field Error

Stepper Motor Test

Stepper motors and Stepper drivers are generally very good at executing repeatable steps that travel a repeatable distance. However, it is always best to double-check rather than assume quality. To test the stepper motors a command of 1000 steps was repeatedly sent to the motor and the distance the ball screw traveled was recorded. All data was taken using a dial gauge contacting the ball nut itself, rather than the 3D printed material stabilizing it. This eliminated any error that the 3D printed material may have introduced. An additional point of note is that this data was taken on the X-Axis Ball screw which at the time of data taking had a slight bow. This may cause the results to show less accuracy than could be achieved with a non-bent screw. A new ball screw has been ordered and will replace the bent screw in the final assembly. It can then be reasonably assumed that the accuracy of the distance traveled may increase with the new equipment.

Errors in probe positioning are converted into field-measurement errors by the local field gradient. The peak and valley of Figure 7 correspond to areas of large gradient, namely at the entrance and exit of the magnet. The resulting field errors (~+/-0.15 mT) are quite low relative to the nominal field of 0.1 T. As these errors are linear in the positioning uncertainty, they are expected to decrease once the integrated system is assembled and all axis are properly aligned and constrained.

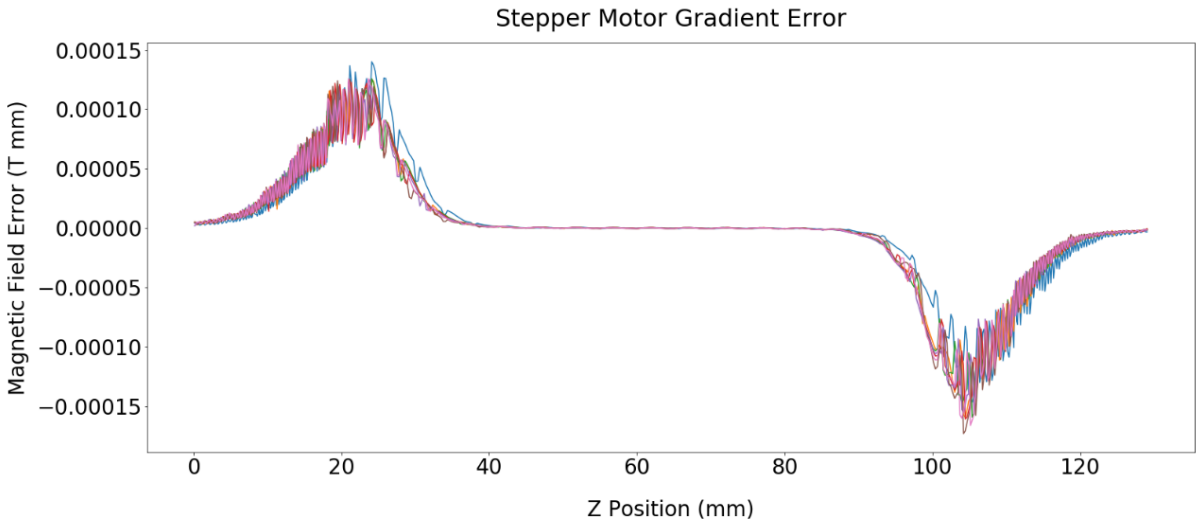

Figure 7. Stepper Motor Gradient Error

Figure 8 shows a histogram of the raw distances traveled in mm of the ball screw when sent 1000 steps. This data can also be seen in Reference Table 1. Four data points from reference table 1 are not shown in the figure 8 plot. These data points fell well outside of the STD of the data set and were excluded from the graph. These four points are expected to be errors in data taking procedure and not in the motors for a few possible reasons. The bend in the ball screw caused the dial gauge to move location on the ball screw as it moved and in a couple of instances, this caused it to catch on or slip to a different surface causing an error in the step distance. This was likely an issue in all data points and will be decreased in the integrated system when properly constrained. Additional all the data points occurred early in the respective runs of their test. This points to an error with the dial gauge where it wasn't reading the full distance traveled accurately until it at reached some threshold of compression of the probe. Overall the standard deviation of the data was ~0.02 mm per 1 mm, resulting in a percent error of ~2% per mm. This positioning error is likely dominated by the lack of rigidity in the temporary mounting components and is expected to improve significantly for the fully assembled system.

Finally, figure 9 shows the integrated field quality of 10,000 simulated scans of the magnetic field affected by the gradient error shown in figure 7. This estimates how positioning errors will result in a deviation of

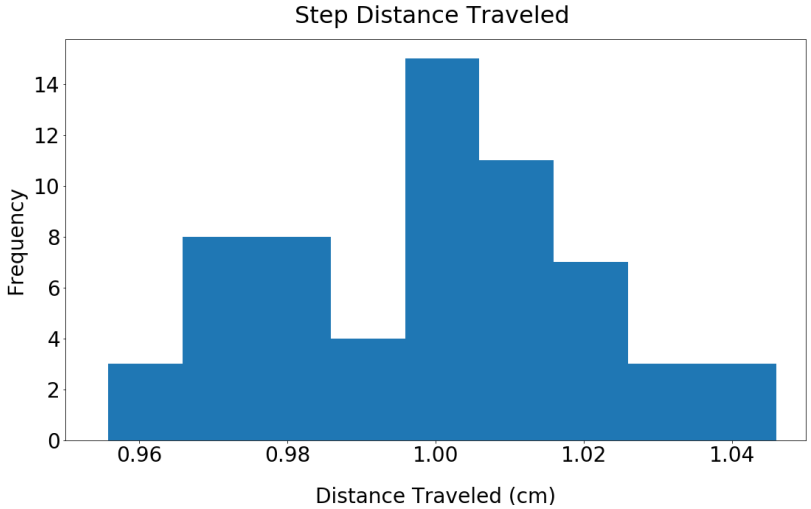

Figure 8. Step Distance Traveled, 1000 Steps = 1 mm

the integrated field when compared to other scans of the same line. Overall the standard deviation of this simulation was 0.0012 T mm and the mean integrated field measurement was 8.836 T mm, resulting in a percent error of 0.0135%; this is on the order of the expected field error due to manufacturing tolerances (cf. figure 6). Considering the limitations of the simple test configuration, this error is quite low and gives confidence that the fully assembled system will be capable of achieving the desired field-mapping precision.

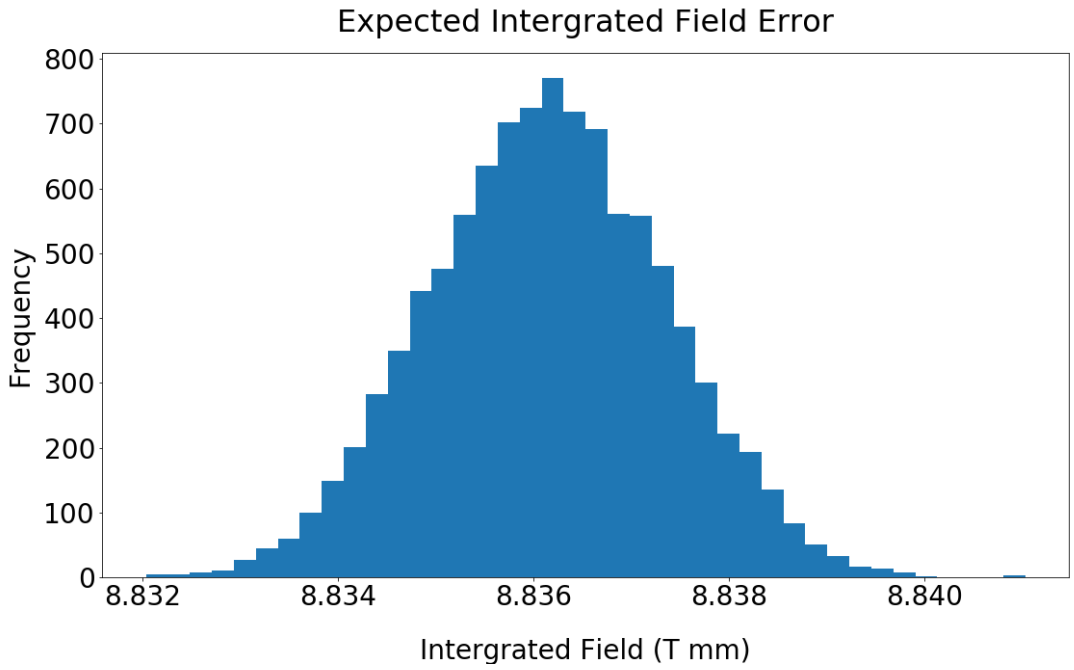

Figure 9. Expected Integrated Field Error

REFERENCES

Part Pictures

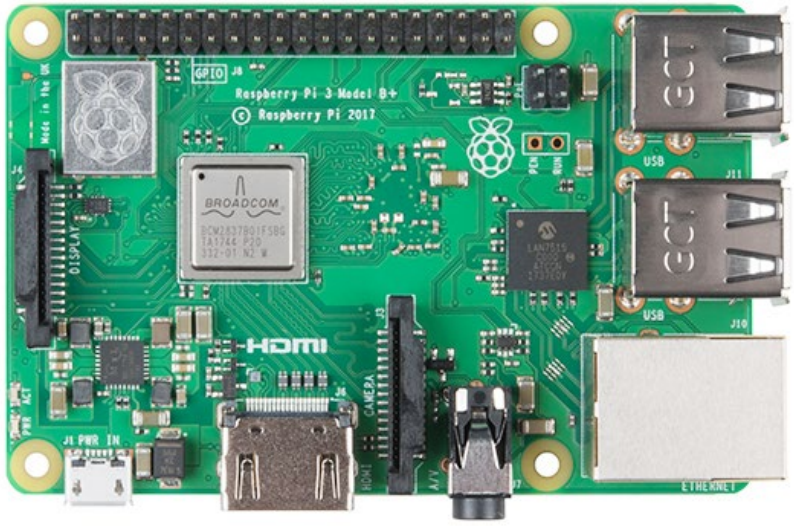

Reference Figure 1. Raspberry Pi 3B+

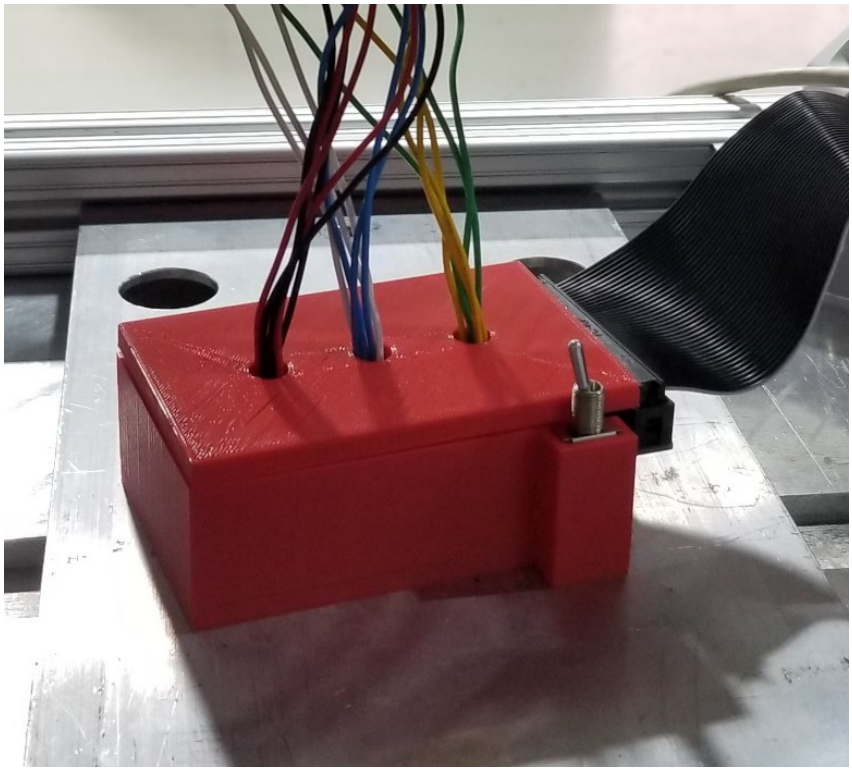

Reference Figure 2. GPIO Breakout Box

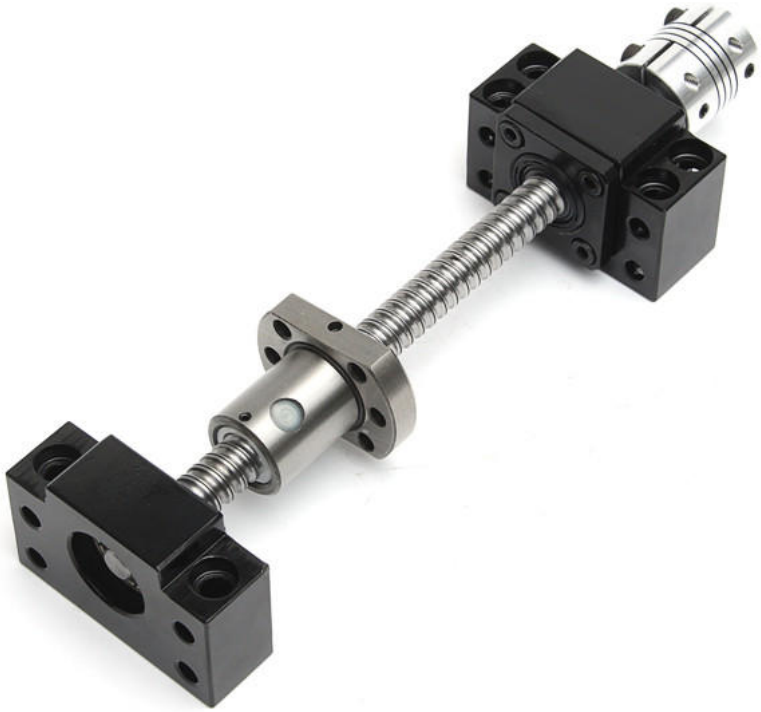

Reference Figure 3. Ball Screw Assembly

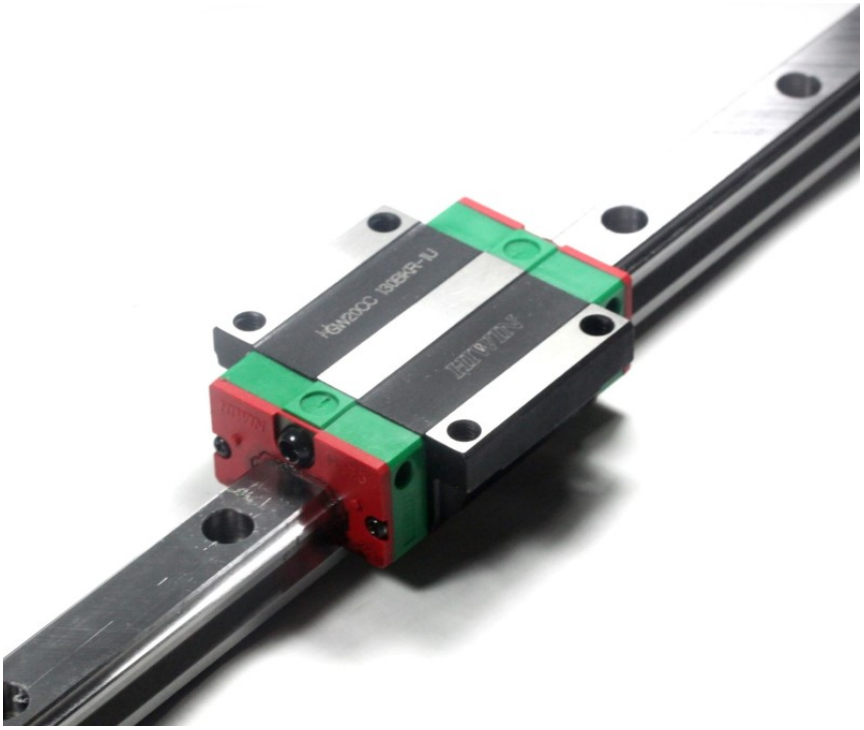

Reference Figure 4. Linear Rail

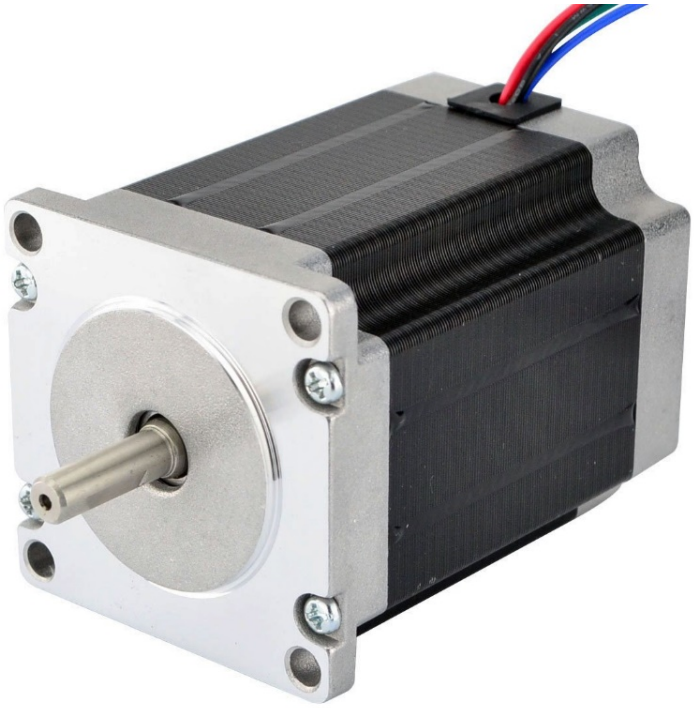

Reference Figure 5. Stepper Motor

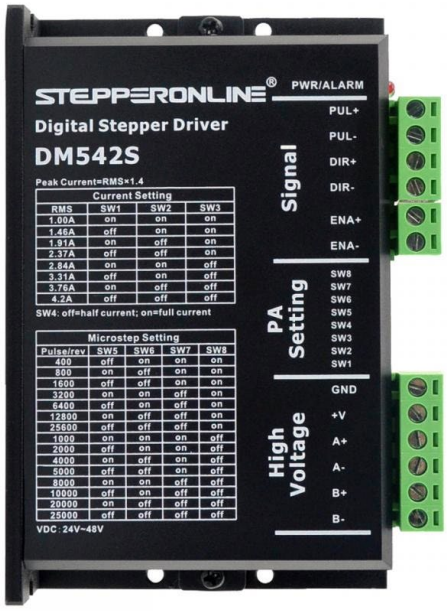

Reference Figure 6. Digital Stepper Driver

Reference Figure 7. 3-Axis Probe

Reference Figure 8. F71 Teslameter

Stepper Motor Test Data

Each data point was taken 1000 steps apart

First Forward Distance	1 F Step (mm)	First Backward Distance	1 B Step (mm)	2F	2 F Step (mm)	2B	2B Step (mm)	3F	3F Step (mm)	3B	3B Step (mm)
0.814	0.814	0.807	0.807	0.77	0.77	0.842	0.842	0.751	0.751	0.816	0.816
1.279	0.465	1.744	0.937	1.814	1.044	1.81	0.968	1.792	1.041	1.796	0.98
1.839	0.56	2.717	0.973	2.528	0.714	2.785	0.975	2.465	0.673	2.776	0.98
2.84	1.001	3.726	1.009	3.515	0.987	3.788	1.003	3.434	0.969	3.798	1.022
3.827	0.987	4.688	0.962	4.524	1.009	4.763	0.975	4.457	1.023	4.763	0.965
4.805	0.978	5.707	1.019	5.565	1.041	5.763	1	5.523	1.066	5.772	1.009
5.803	0.998	6.708	1.001	6.621	1.056	6.777	1.014	6.53	1.007	6.777	1.005
6.766	0.963	7.675	0.967	7.539	0.918	7.753	0.976	7.455	0.925	7.769	0.992
7.794	1.028	8.697	1.022	8.545	1.006	8.761	1.008	8.465	1.01	8.769	1
8.764	0.97	9.674	0.977	9.552	1.007	9.748	0.987	9.497	1.032	9.748	0.979
9.742	0.978	10.673	0.999	10.583	1.031	10.753	1.005	10.52	1.023	10.752	1.004
10.754	1.012	11.676	1.003	11.602	1.019	11.756	1.003	11.517	0.997	11.771	1.019
11.726	0.972	12.687	1.011	12.519	0.917	12.753	0.997	12.443	0.926	12.755	0.984
12.725	0.999										

Reference Table 1. Stepper Motor Test Data

Links to Parts

Raspberry Pi 3b+ : https://www.raspberrypi.org/products/raspberry-pi-3-model-b-plus/

CNC Kit: https://www.vxb.com/4-X2-Feet-CNC-Router-Kit-Rail-Guide-System-p/4x2-feet-cnc-linear-guide-kit.htm

F71 Teslameter and Probe: https://www.lakeshore.com/products/categories/overview/magnetic-products/gaussmeters-teslameters/f71-and-f41-teslameters

Stepper Driver: https://www.omc-stepperonline.com/dm542s.html

Stepper Motor: https://www.omc-stepperonline.com/nema-23-bipolar-18deg-19nm-269ozin-3a-336v-57x57x76mm-4-wires-23hs30-3004s.html

ACKNOWLEDGMENTS

I would like to express my very great appreciation to Jonathan Jarvis for his continued support and expertise during this project. His willingness to give his time so generously has been very much appreciated. Additional thanks for assistance provided by Dave Franck and Peter Garbincius which was greatly appreciated. Finally, my special thanks to Jamie Santucci for some great tours.